IEEE Access
Multidisciplinary | Rapid Review | Open Access Journal

Received June 6, 2020, accepted July 2, 2020, date of publication July 27, 2020, date of current version August 6, 2020.

Digital Object Identifier 10.1109/ACCESS.2020.3012040

Optimizing CdZnTeSe Frisch-Grid Nuclear Detector for Gamma-Ray Spectroscopy

STEPHEN U. EGARIEVWE[1], (Member, IEEE), UTPAL N. ROY[2,3], EZEKIEL O. AGBALAGBA[4], BENICIA A. HARRISON[5], CARMELLA A. GOREE[6], EMMANUEL K. SAVAGE[7], AND RALPH B. JAMES[2], (Fellow, IEEE)

[1]Nuclear Engineering and Radiological Science Center, Alabama A&M University, Huntsville, AL 35811, USA
[2]Savannah River National Laboratory, Science and Technology Directorate, Aiken, SC 29808, USA
[3]Brookhaven National Laboratory, Department of Nonproliferation and National Security, Upton, NY 11973, USA
[4]Department of Physics, Federal University of Petroleum Resources, Effurun 922104, Nigeria
[5]College of Medicine, University of South Alabama, Mobile, AL 36688, USA
[6]Biological and Environmental Sciences Department, Alabama A&M University, Huntsville, AL 35811, USA
[7]Department of Physics, Chemistry, and Mathematics, Alabama A&M University, Huntsville, AL 35811, USA

Corresponding author: Stephen U. Egarievwe (stephen.egarievwe@aamu.edu)

This work was supported in part by the U.S. Department of Energy, Office of Defense Nuclear Nonproliferation Research and Development, DNN R&D (NA-22); in part by the National Science Foundation (NSF) HBCU-UP Program through award number 1818732; in part by the NSF Louis Stokes Alliances for Minority Participation (LSAMP); and in part by the U.S. Nuclear Regulatory Commission (NRC) through awards number 31310018M0035.

ABSTRACT Wide bandgap semiconductor materials capable of detecting X-rays and gamma-rays at room temperature without cryogenic cooling have great advantages that include portability and wide-area deployment in nuclear and radiological threat defense. Additional major applications include medical imaging, spectroscopy, and astrophysics. Most current room-temperature ionizing radiation detector devices are fabricated from cadmium telluride (CdTe) and cadmium zinc telluride (CdZnTe). Cadmium zinc telluride selenide (CdZnTeSe or CZTS) can be grown with high crystal yield compared to CdTe and CdZnTe. Thus, CZTS has the advantage of lowering the cost of room-temperature nuclear detectors. Thick CdTe-based detectors are prone to the trapping of charge carriers, thus limiting energy resolution and efficiency. A Frisch-Grid configuration helps to solve this problem. This research is focused on optimizing the Frisch-grid configuration for a CZTS detector. The CZTS was grown by traveling heater method. Infrared images of the CZTS matrix largely showed the absence of tellurium inclusions. The resistivity of the CZTS obtained from a current-voltage plot is of the order of 10^{10} Ω.cm. The charge-transport characterized by measuring the electron mobility-lifetime product is 4.7×10^{-3} cm^2/V. Detector resolution was measured for various Frisch-ring widths. For a $4.8 \times 4.9 \times 9.7$ mm^3 detector, the best Frisch-ring widths were found to be 3-4 mm. A detector resolution of 1.35% full-width-at-half-maximum was obtained for the 3-mm width at −2300 V bias voltage for the 662-keV gamma peak of ^{137}Cs. A resolution of 1.36% was obtained for the 4-mm width at −1800 V applied bias.

INDEX TERMS CdZnTeSe detectors, detector resolution, Frisch-grid, gamma-ray detector, nuclear radiation detector, traveling heater method, X-ray detector.

I. INTRODUCTION

Semiconductor photonic materials capable of detecting X-rays and gamma-rays at room temperature without cryogenic cooling have great advantages that include portability and wide-area deployment in nuclear and radiological threat defense. Additional specific applications include medical imaging, spectroscopy, and astrophysics [1]–[5]. The most prominent of these wide-bandgap semiconductors are cadmium telluride (CdTe) and cadmium zinc telluride (CdZnTe). These materials are however prone to low detector yield due to defects that are related to Te inclusions, sub-grain boundary network, precipitates and nonuniform composition [6]–[8]. This in turn leads to a relatively high cost of X-ray and gamma-ray detection devices built from CdTe and CdZnTe materials. A major effort at reducing the defects and increasing the crystal growth yield is to grow CdTe-based materials that have greater uniformity in the crystal structure.

The associate editor coordinating the review of this manuscript and approving it for publication was Baile Chen.

One approach to growing CdTe-based materials with high crystal uniformity is to include elements such as Mn and Se that have segregation coefficients of ∼1.0 in CdTe matrix. This has led to efforts to develop crystals such as cadmium manganese telluride (CdMnTe) [9]–[15] and cadmium telluride selenide (CdTeSe) [16], [17]. Recently, Roy *et al.* spearheaded efforts in the development of the quaternary compound cadmium zinc telluride selenide (CdZnTeSe or CZTS). The group reported high crystal uniformity, absence of performance-limiting defects that often plague CdTe and CdZnTe, and high energy resolution for gamma rays [18]–[34]. Selenium, when added to the CdTe matrix, is very effective in reducing defects related sub-grain boundary networks, Te inclusions and precipitates [18], [19]. Roy *et al.* experimented with the growth of CZTS using two techniques: vertical Bridgman method and the traveling heater method (THM). Comparative assessments of the CZTS material and detector properties supported the THM method as the preferred approach due to the following advantages [18], [19]:

- THM occurs at much lower temperature than Bridgman Method.
- THM has less chance of incorporation of impurities from the crucible during growth.
- THM has less chance of ampoule explosion during the growth process.
- THM allows for an enhanced purity of the ingot.
- THM-grown crystals have fewer defects due to the lower growth temperature.

In our studies using photo-induced current deep-level transient spectroscopy (iDLTS), we found that Bridgman-grown CZTS showed a high density of the 1.1-eV trap compared to the absence of the 1.1-eV trap in THM-grown CZTS [20], [21]. As a result of trapping by this deep trap, the Bridgman-grown CZTS detector showed no response to gamma rays, even with its high resistivity of 2×10^{10} Ω.cm [21]. On the contrary, THM-grown CZTS detector showed good response to gamma rays. Table 1 shows the energy resolutions, measured as full-width-at-half-maximum (FWHM) of the photopeak, for CZTS Frisch-grid detectors fabricated from $Cd_{0.9}Zn_{0.1}Te_{0.98}Se_{0.02}$ crystal grown by THM [22], [32].

An energy resolution of 0.9% was recorded at −1800 V applied bias for a CZTS Frisch-grid detector fabricated from a recent crystal grown by THM [32]. The composition of the CZTS is very important in the crystal growth process. The path taken to growing CZTS crystals is to have a compound that could match the CZT bandgap (approximately 1.57 eV for 10 at% Zn) while keeping Se at ∼7 at% [23]. This approach is based on observation that 7 at% for Se in CdTe matrix is most effective in reducing Te inclusions and sub-grain boundary networks while giving high compositional homogeneity [24]. The concentration of Zn was kept at ∼10 at% while varying Se from 2 to 7 at% in an optimization procedure to lower the amount of Te inclusions and precipitates [23]. A compositional study showed that the bandgap of CZTS was more uniform than CZT for THM-grown crystals [24]. The 7% Se CZTS was uniform along the length of the ingot, and only a slight bandgap variation was observed for 2% and 4% Se in regions that are less than 1 cm near the interface [24].

TABLE 1. Energy resolutions of CZTS Frisch-grid detectors fabricated from THM-grown crystals by Roy *et al.* [22], [32].

Radiation Source	γ-Peak (MeV)	Resolution (FWHM)	Shaping Time (μs)	Applied Bias[a] (V)	Detector Size (mm^3)
^{167}Cs	0.662	1.3%	6	1800	3.6 x 3.4 x 9.7
^{167}Cs	0.662	0.9%	2	1800	5.0 x 5.0 x 12.3
^{167}Cs	0.662	1.08%	2	3000	4.5 x 4.5 x 10.8
^{133}Ba	0.031	6.4%	2	3000	4.5 x 4.5 x 10.8
^{133}Ba	0.081	4.8%	2	3000	4.5 x 4.5 x 10.8
^{133}Ba	0.276	1.77%	2	3000	4.5 x 4.5 x 10.8
^{133}Ba	0.303	1.7%	2	3000	4.5 x 4.5 x 10.8
^{133}Ba	0.356	1.75	2	3000	4.5 x 4.5 x 10.8
^{60}Co	1.17	1.2%	6	1800	3.6 x 3.4 x 9.7
^{60}Co	1.33	1.0%	6	1800	3.6 x 3.4 x 9.7
^{22}Na	0.511	1.8%	6	1800	3.6 x 3.4 x 9.7
^{22}Na	1.2	1.0%	6	1800	3.6 x 3.4 x 9.7

Crystal composition: $Cd_{0.9}Zn_{0.1}Te_{0.98}Se_{0.02}$.
[a]Negative bias voltage.

The technical challenges in the development of CZTS are mainly in growing large-diameter ingots, achieving high resistivity, and getting high mobility-lifetime ($\mu\tau$) product for the charge carriers [25]. The resolutions for some of these technical challenges include: 1) using seeded growth to increase the grain size of the ingots; 2) purification of the starting materials, especially cadmium selenide (CdSe); 3) increasing the resistivity through the alloy composition or compensation process; and 4) increasing the number of growth furnaces to get a faster optimization and development output.

We grew $Cd_{0.9}Zn_{0.1}Te_{0.98}Se_{0.02}$ by THM to perform charge transport studies and recorded an electron $\mu\tau$-product of $\sim 4 \times 10^{-3}$ cm^2/V for a $6.35 \times 4.33 \times 2.48$ mm^3 planar detector fabricated from an as-grown ingot [27]. The resistivity was 2×10^{10} Ω.cm and an energy resolution of 11% FWHM was observed for the 59.6-keV gamma line of ^{241}Am, at 170 V applied bias [27].

The surface current is an important factor in determining the energy resolution since it contributes to electronic noise. Chemical passivation is often used to stabilize the surfaces of CdTe-based detectors, and also minimize surface oxidation and increase the shelf life of the devices [35]–[37]. In our chemical passivation studies on one of our recent CZTS ($Cd_{0.9}Zn_{0.1}Te_{0.96}Se_{0.04}$ grown by THM) using 10% aqueous solution of ammonium fluoride, we found an average of 25% improvement in the resolution of a planar detector ($7.00 \times 4.65 \times 2.70$ mm^3) for the 59.6-keV gamma line of ^{241}Am at bias voltages in the range −35 V to −200 V [29]. The highest improvement of 33% (from 17.9% to 12.0% FWHM) was recorded at −35 V, and the smallest improvement was 19% (from 9.9% to 8.0% FWHM) at −100 V applied bias [29].

The best energy resolution of 6.4% FWHM was recorded at −180 V applied bias [29].

Bezsmolnyy [38] studied the electrophysical properties of chlorine-doped $Cd_{1-x}Zn_xTe_{1-y}Se_y$ (with compositions in the range x = 0.005 to 0.02 and y = 0.02 to 0.045) grown by the vertical Bridgman method. The resistivity ranged from 10^8 to 10^9 Ω.cm, and the $\mu\tau$-product was 1.8×10^{-3} cm^2/V for electrons and 2.0×10^{-4} cm^2/V for holes [38]. An energy resolution of 9 keV FWHM was recorded for the 59.6-keV gamma line of ^{241}Am at 300 K [38].

Our recent studies have shown that CZTS has the advantage of lowering the cost of room-temperature nuclear detection devices. In particular, the addition of Se to the CZT matrix significantly reduced Zn segregation, limited the formations of sub-grain boundaries and their networks, limited the formation of Te inclusions and precipitates, and improved the compositional homogeneity of the CZTS matrix [31]. Optical photograph and X-ray topographic image on a 2-inch diameter $Cd_{0.9}Zn_{0.1}Te_{0.93}Se_{0.07}$ grown by THM showed the complete absence of sub-grain boundary networks, and there were very few sub-grain boundaries, much less than often present in CZT [31]. The average concentration of Te inclusions (∼2.5×10^5 cm^{-3}) was found to be about one order of magnitude less than that in CZT grown by a similar technique [31]. This evidence of better material quality often translates to higher detector performance, increased detector yield and a lower cost of production. Another advantage of CZTS is in microhardness. Franc *et al.* [39] recently reported a higher microhardness in CZTS crystals than CZT.

In this report, we present the characterization of a CZTS Frisch-grid detector fabricated from an as-grown crystal grown by THM. We present the steps taken to optimize the Frisch-ring width and the energy resolution of the detector. The detectors were tested using ^{137}Cs, ^{133}Ba and ^{22}Na nuclear radiation sources.

II. VIRTUAL FRISCH-GRID DETECTOR

The virtual Frisch-grid detector configuration is used to reduce fluctuations in device response to incoming γ-rays and X-rays, thereby improving the energy resolution compared to a simple planar geometry [40]–[43]. The schematic of the Frisch-grid configuration used in this study is shown in Fig. 1.

The fabrication of Frisch-grid detectors are extensively described in [40]–[43]. Incoming photons produce charge carriers that drift to the electrodes (electrons to the anode and holes to the cathode). The induced charge at the electrodes depends largely on the complete drift of the charge carriers to the electrode. The trapping of charge carriers results in an inability to collect all charges created [40], and thus leads to fluctuations in the induced charge. According to McGregor *et al.* [40] the Frisch-grid configuration greatly reduces the influence of the photon interaction region on the pulse shape. McGregor *et al.* [40] studied the effect of a parallel Frisch-grid on a $5 \times 2 \times 5$ mm^3 CdZnTe using ^{137}Cs at an applied bias of −80 V. It was observed that the 662-keV gamma peak did not show in the spectrum with the grid turned off, but an energy resolution of 6.2% FWHM was recorded with the grid turned on [40]. The effects of the Frisch-ring width on long (> 15 mm) CdZnTe detectors was studied by Polack *et al.* [42], where they showed that the width can be safely reduced to 3 mm without diminishing its effectiveness. The optimal Frisch-grid width for a $6 \times 6 \times 15$ mm^3 was found to be ∼5-6 mm [42].

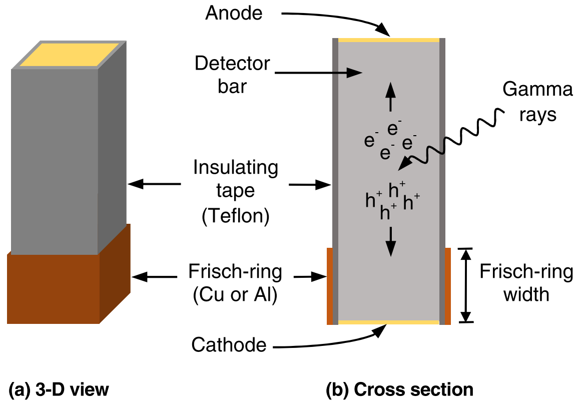

FIGURE 1. Schematic of virtual Frisch-grid detector configuration. Not drawn to scale. Electrons (e$^-$) drift towards the anode and holes (h$^+$) drift towards the cathode.

III. EXPERIMENTS

The experiments focus on characterizing CZTS Frisch-grid detectors and systematically varying the Frisch-grid width to obtain its optimum value for a ∼$4.8 \times 4.9 \times 9.7$ mm^3 detector bar using a ^{137}Cs radiation source. After establishing the optimum width, we carried out further experiments to determine the optimum applied bias voltage. This was following by determining the optimum shaping time for the optimum width and applied bias voltage. The spectra for ^{133}Ba and ^{22}Na gamma sources were also recorded.

A. DETECTOR MATERIAL AND FABRICATION

The ∼$4.8 \times 4.9 \times 9.7$ mm^3 Frisch-grid detector was fabricated from an as-grown $Cd_{0.9}Zn_{0.1}Te_{0.98}Se_{0.02}$ ingot. It was grown by THM in a Te-rich solution and with indium doping. The CZTS was grown from very high purity materials. These include 6N-purity CdZnTe and CdSe. The indium and Te were also of 6N purity. The details of the growth technique are described in [31].

The $4.8 \times 4.9 \times 9.7$ mm^3 bar was cut from the as-grown CZTS ingot using a programmable diamond-impregnated wire saw. The CZTS bar was then successively polished using silicon carbide abrasive papers, starting with 800-grit to a finer 1200-grit paper. The surfaces of the bar were further smoothened by polishing on MultiTex pads with alumina powder. The sizes of the alumina powder were successively varied from 3.0 to 0.1 μm. Residues from the polishing were removed by rinsing the bar with distilled water. This was followed by drying with compressed nitrogen.

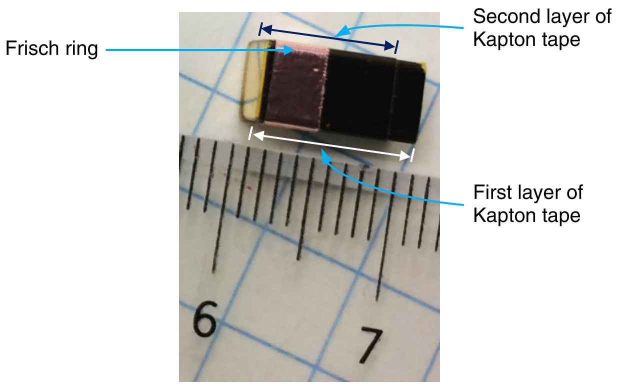

FIGURE 2. The 4.8 × 4.9 × 9.7 mm^3 Frisch-grid detector fabricated from an as-grown $Cd_{0.9}Zn_{0.1}Te_{0.98}Se_{0.02}$ ingot.

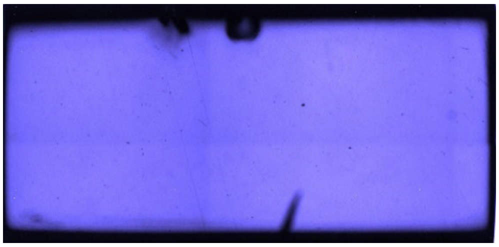

FIGURE 3. Infrared image near the surface on a 4.78 × 9.70 mm^2 side. It is a composite of six images stitched together by the software that comes with the Nikon Eclipse LV100 microscope. The object near the center at the bottom is a marker for tracking placement orientation.

The next phase in the Frisch-grid detector fabrication process is the deposition of electrical contacts (electrodes) on the two opposite ∼4.8 × 4.9 mm^2 sides of the parallelepiped-shaped bar. This was accomplished by depositing gold contacts using the electroless deposition technique [35], [43], [44]. Our electroless deposition process for each electrode involved pipetting the solution of gold chloride ($AuCl_3$) onto the CZTS surface for each electrode. An appropriate amount of $AuCl_3$ was used to cover the surface while avoiding spills over the edges. After reaction with the surface, we removed excess $AuCl_3$ solution using a felt paper. The felt paper draws the excess solution without touching the CZTS surface. The sample was then rinsed with distilled water and dried with compressed nitrogen. Next, the walls of the sample were tightly wrapped with a double layer of thin insulating Kapton tape (see Fig. 1). The first layer covered the entire 9.7-mm length of the sample. The second layer covered ∼7 mm, the maximum Frisch ring used in the present case (see Fig. 2). Alternative materials often used for the insulating layer are ultra-thin polyester [41] and Teflon tape [46]. After the application of an insulating layer on the walls, the Frisch-ring was made by tightly wrapping a self-adhesive thin cooper foil on the cathode side of the walls (see Figs. 1 and 2). The Frisch-grid CZTS detector is shown in Fig. 2.

B. DETECTOR CHARACTERIZATION

Infrared transmission imaging was performed on the CZTS sample after polishing the surfaces to a mirror-shine finish prior to the deposition of the gold electrical contacts.

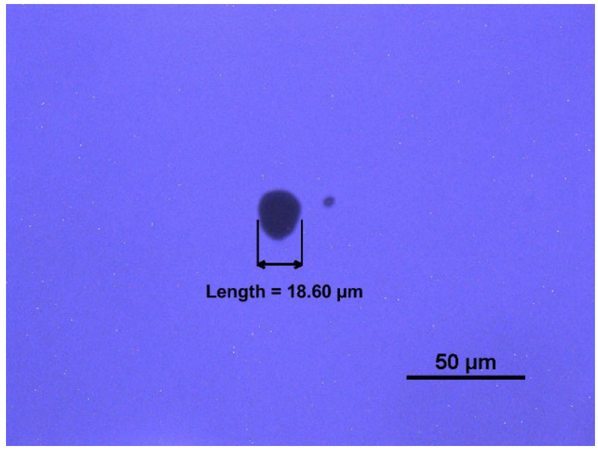

(a)

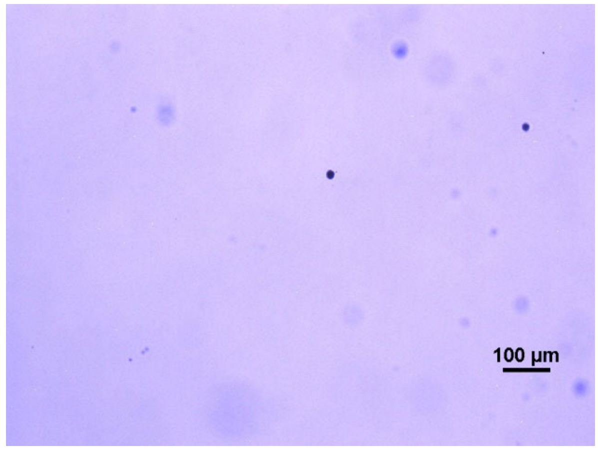

(b)

FIGURE 4. High-magnification infrared images showing Te inclusions in very few areas of the mostly Te inclusion free CZTS sample. (a) An area of about 247 × 185 μm^2 showing only one large Te inclusion and relatively small inclusion. (b) A larger area (lower magnification) showing very few Te inclusions.

The infrared transmission imaging system consists of a Nikon Eclipse LV100 microscope fitted with an infrared light source, a camera, and a motorized stage with xyz-translation capability. The microscope is equipped with a software for capturing and analyzing the image. The infrared image recorded near the surface on one of the ∼4.8 × 9.7 mm^2 sides of the sample is shown in Fig. 3.

Several infrared images of the CZTS matrix largely showed the absence of Te inclusions and grain boundaries. Very few Te inclusions were observed in some areas (see Fig. 4). In Fig 4a, only one large Te inclusion of ∼18.6-μm diameter was observed in an area of about 247 × 185 μm^2. The infrared image of a larger area is shown in Fig. 4b. The Te inclusion may be associated with instabilities at localized regions of the growth interface that lead to the entrapment of Te [32], and it is very common in CdZnTe grown by THM [47].

Current-voltage (I-V) measurements were made on the CZTS sample after the deposition of the gold electrical contacts. The sample was mounted in a customized aluminum

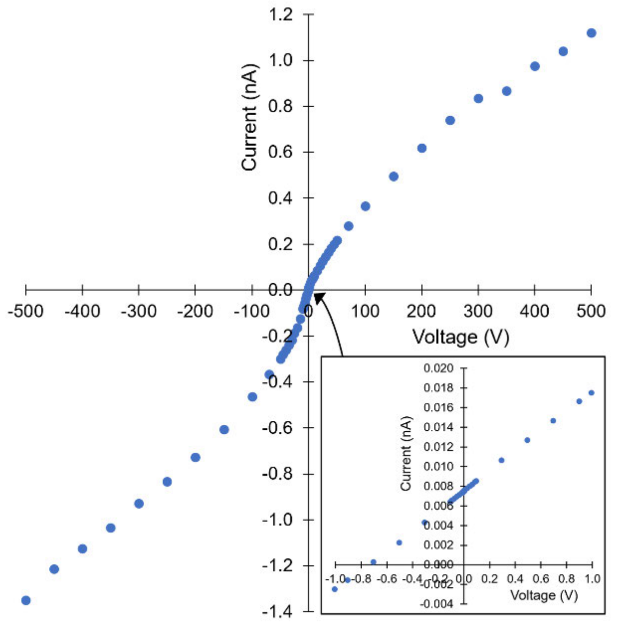

FIGURE 5. I-V plot of the CZTS detector before fabricating into a Frisch-grid geometry. The offset in the insert is from the Keithley Picoammeter.

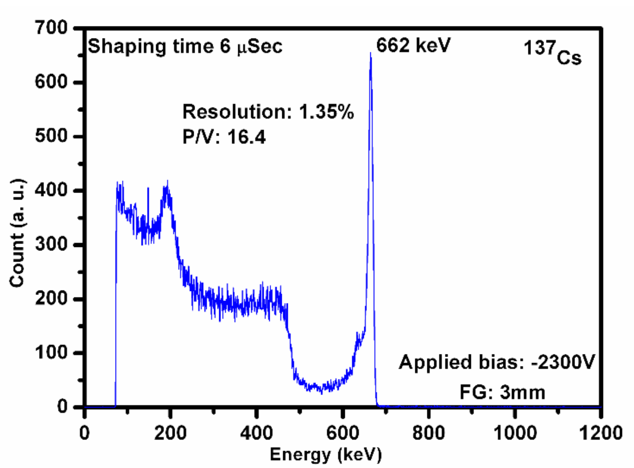

FIGURE 6. Spectrum of ^{137}Cs obtained at room temperature from a 4.8 × 4.9 × 9.7 mm^3 CZTS Frisch-grid detector with a Frisch ring of 3-mm width. P/V is peak-to-valley ratio for the 662-keV gamma line.

box fitted with BNC and connected to a Keithley Picoammeter and Voltage Source model 6487. The applied voltages were in the range of −500 V to 500 V. The I-V plot is shown in Fig. 5. The resistivity of the CZTS obtained from the I-V plot is of the order of 10^{10} Ω.cm.

Radiation detection measurements were made using a special sample holder built by eV Products (now Kromek). The holder is fitted with a beryllium window on which the sealed radiation source is placed. It is connected to a variable high-voltage supply. The signal from the sample holder passes through a preamplifier and an amplifier to a multichannel analyzer (MCA). The MCA is connected to a computer with a software that records the radiation spectrum.

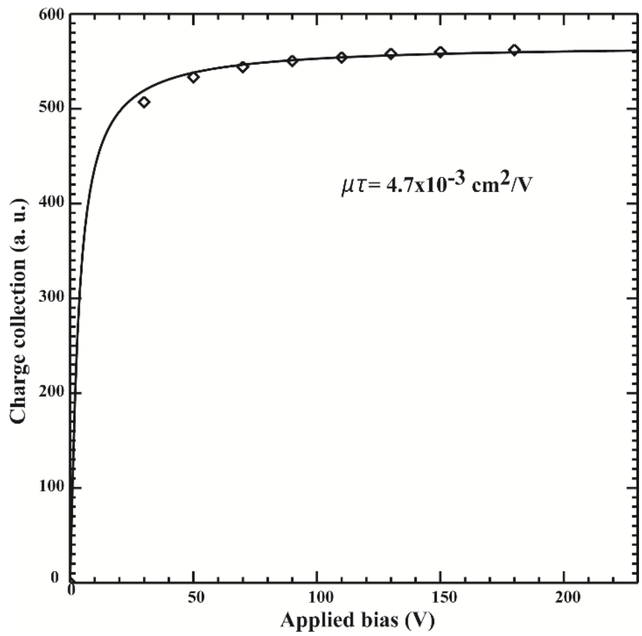

FIGURE 7. Plot of charge collections at various applied voltages and fitting of the Hecht equation to determine the electron mobility-lifetime $(\mu\tau)_e$ product. The charge collection was recorded for the 59.6-keV gamma peak of ^{241}Am.

TABLE 2. Best energy resolutions for various Frisch-ring widths.

Frisch-Ring Width (mm)	Applied Voltage[a] (V)	Shaping Time (μs)	Resolution (FWHM)
2	1500	6	1.46%
3	2300	6	1.35%
4	1800	6	1.36%
5	2000	6	1.84%
6	2400	6	1.87%
7	2300	6	2.35%

[a]Negative bias voltage.

The spectrum of ^{137}Cs obtained at room temperature from a CZTS Frisch-grid detector with a Frisch ring of 3-mm width is shown in Fig. 6. The energy resolution for the 662-keV gamma line is 1.35% (as estimated from Gaussian fitting), and the peak-valley (P/V) ratio is 16.4.

The charge-transport of the CZTS material was characterized by determining the electron mobility-lifetime $(\mu\tau)_e$ product using a planar detector as shown in Fig. 7. This was obtained from recording the charges collected at various applied voltages and fitted to the Hecht equation [48], [49]. The data for Fig. 7 was obtained by placing an ^{241}Am sealed radiation source close to the cathode side of the planar detector. The charge collection was recorded for the 59.6-keV peak of ^{241}Am. The $(\mu\tau)_e$ product is 4.7×10^{-3} cm^2/V.

C. OPTIMIZATION OF THE FRISCH-RING WIDTH

The width of the Frisch-ring greatly affects the performance of the detector. Hence, it is important to optimize the width, which could be different for each detector material and size.

TABLE 3. Energy resolutions for various Frisch-ring widths.

Frisch-Ring Width (mm)	Applied Voltage[a] (V)	Shaping Time (μs)	Resolution (FWHM)
2	1000	6	1.66%
2	1500	6	1.46%
2	1800	6	1.57%
2	2000	6	1.48%
2	2200	6	1.55%
2	2400	6	1.78%
3	1000	6	1.77%
3	1200	6	1.66%
3	1400	6	1.50%
3	1600	6	1.49%
3	1800	6	1.46%
3	1900	6	1.47%
3	2000	6	1.36%
3	2300	6	1.35%
3	2400	6	1.55%
3	2300	3	1.95%
3	2300	2	2.25%
3	2300	1	1.80%
4	1000	6	1.55%
4	1200	6	1.50%
4	1400	6	1.50%
4	1500	6	1.50%
4	1600	6	1.54%
4	1800	6	1.36%
4	2000	6	1.52%
4	2200	6	1.93%
4	1000	3	2.18%
4	1800	3	1.85%
5	1800	6	1.85%
5	1900	6	1.90%
5	2000	6	1.84%
5	2100	6	1.96%
5	2200	6	2.05%
5	2300	6	2.40%
5	2200	3	2.37%
5	2300	3	2.61%
6	2300	6	2.33%
6	2400	6	1.87%
6	2500	6	2.18%
6	2300	3	2.37%
6	2400	3	2.14%
6	2400	2	2.23%
6	2400	1	2.44%
6	2400	0.5	2.80%
7	2200	6	2.76%
7	2300	6	2.35%
7	2400	6	2.75%
7	2300	3	4.10%

[a]Negative bias voltage.

For the CZTS used in this experiment, the width of the Frisch-ring was varied from 2 mm to 7 mm. The optimum applied voltage and shaping time for the best energy resolution were systematically determined for each Frisch-ring width using a ^{137}Cs source. A coarse gain of 100 and acquisition time of 300 seconds were used for all measurements.

IV. RESULTS AND DISCUSSION

A. CZTS FRISCH-GRID DETECTOR

The best resolutions for the Frisch-ring widths are shown in Table 2. The best resolutions obtained are 1.35% for the 3-mm Frisch-ring width at a bias voltage of −2300 V, and

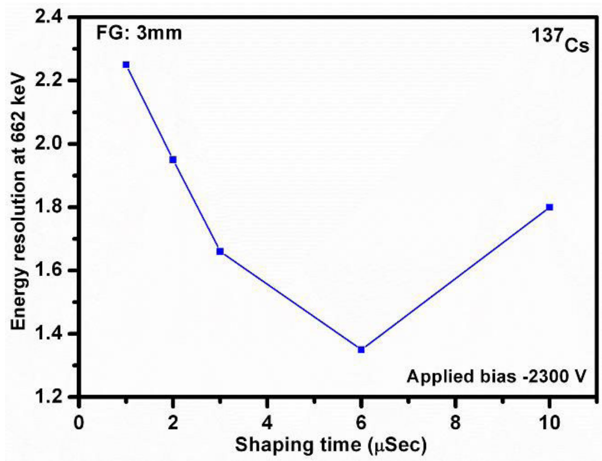

FIGURE 8. Plot of energy resolution versus the amplifier shaping time for the Frisch-ring of 3-mm width.

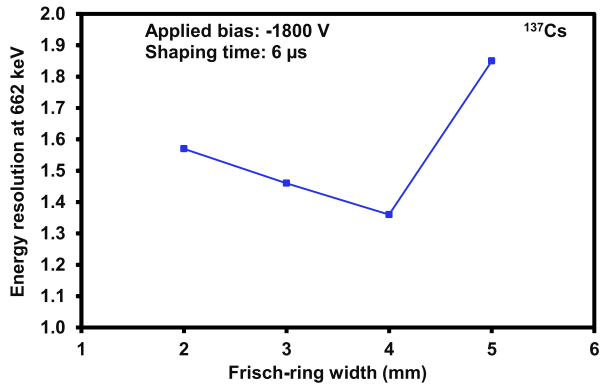

FIGURE 9. Plot of energy resolution versus Frisch-ring width at 6 μs amplifier shaping time and −1800 V applied bias. The spectra at −1800 V for 6-mm and 7-mm Frisch ring widths were much worst.

1.35% at −1800 V for the 4-mm width. For each Frisch-ring width, the applied voltage is varied together with the shaping time of the amplifier to get the best resolution. The detailed results are shown in Table 3. The 6-μs shaping time gave the best energy resolution for the Frisch-ring widths. This is shown in Fig. 8 for the 3-mm width at an applied voltage of −2300 V.

The plot of energy resolution versus Frisch-ring width at 6 μs amplifier shaping time and −1800 V applied bias is shown in Fig. 9. We did not record the spectra at −1800 V for 6-mm and 7-mm Frisch-ring widths because the resolutions were much worst. The spectrum for a ^{133}Ba source obtained at an applied voltage of −1800 V for a 4-mm-wide Frisch ring is shown in Fig. 10, and that for a ^{22}Na source is shown in Fig. 11. The energy resolutions for the 81-keV peak of ^{133}Ba is 9.45% and that of the 356-keV peak is 2.6%. The energy resolution for the 511-keV peak of ^{22}Na is 1.75% and that of the 1.275-MeV peak is 1.2%.

B. COMRARISON OF CZTS TO CZT

The key difference between CZTS and its major counterparts, CdTe, and CZT, is the ability of Se to effectively prevent

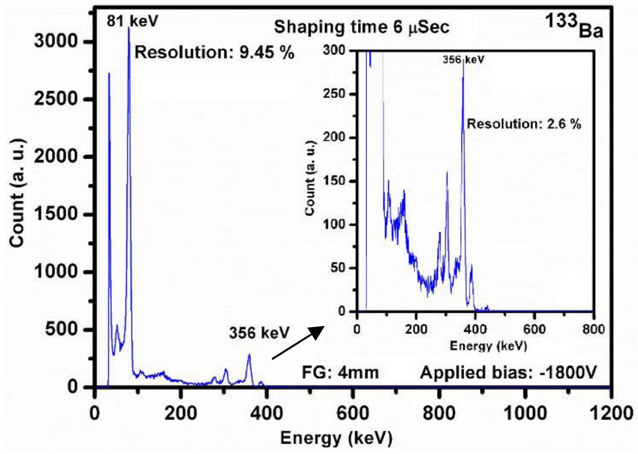

FIGURE 10. Spectrum of ^{133}Ba obtained at room temperature from a 4.78 × 4.90 × 9.70 mm^3 CZTS Frisch-grid detector with a Frisch-ring of 4-mm width.

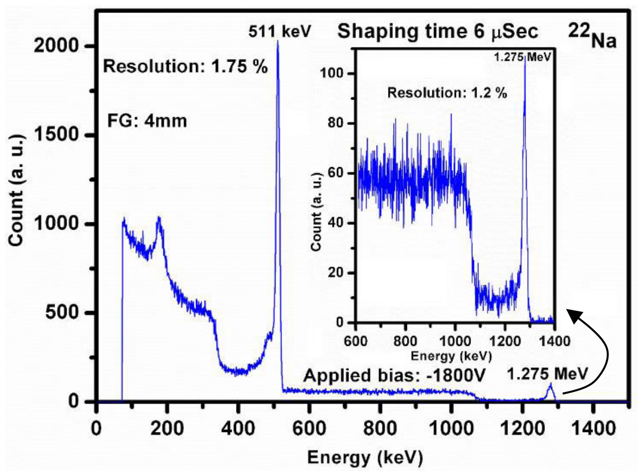

FIGURE 11. Spectrum of ^{22}Na obtained at room temperature from a 4.78 × 4.90 × 9.70 mm^3 CZTS Frisch-grid detector with a Frisch-ring of 4-mm width.

sub-grain boundary networks from being formed during the crystal growth process [32]. The segregation coefficient of Zn in CdTe matrix is >1 and is significantly reduced by Se [31]. Thus, the presence of Se leads to better crystal compositional uniformity, and hence higher yield of defect-free regions in the ingot and better detector resolution.

The $4.8 \times 4.9 \times 9.7$ mm^3 CZTS Frisch-grid detector in this study has a resolution of 1.35% for the 662-keV gamma peak of ^{137}CS at −2300 V applied voltage. Roy *et al.* [32] obtained a resolution of 0.9% at −1800 V applied voltage for a $5.0 \times 5.0 \times 12.3$ mm^3 CZTS Frisch-grid detector. Polack *et al.* [42] reported the optimal Frisch-grid width for a $6 \times 6 \times 15$ mm^3 CZT detector to be ∼5-6 mm. The measured resolution for the CZT Frisch-grid detector before and after charge-loss correction were ∼3.7% and 1.1% respectively [42]. Charge-loss correction was not applied to the 1.35% recorded here as well as for the 0.9% resolution reported by Roy *et al.* [32] for CZTS Frisch-grid detectors. As-measured resolution of 2% was reported by Bolotnikov *et al.* [50] for a $6 \times 6 \times 20$ mm^3 CZT Frisch-grid detector.

V. CONCLUSION

We have characterized a $4.8 \times 4.9 \times 9.7$ mm^3 CZTS Frisch-grid detector and systematically determined that the Frisch-ring widths of 3 mm and 4 mm gave the best energy resolutions. The best resolution obtained for the ^{137}Cs 662-keV gamma lines is 1.35% for the 3-mm Frisch-ring width at a bias voltage of −2300 V, and the best resolution of 1.36% at −1800 V was obtained for the 4-mm-wide ring. No electronic corrections were made to compensate for electron trapping or non-uniformities in the electron charge collection. It is expected that the optimum Frisch-ring width will be different for different detector heights. Polack *et al.* [42] reported the optimal Frisch-grid width for a $6 \times 6 \times 15$ mm^3 CdZnTe to be ∼5-6 mm.

The 4-mm-wide Frisch ring has an advantage over the 3-mm width because of its lower operating voltage for similar energy resolutions. At 6-μs shaping time, the same energy resolution of 1.55% was obtained for the 4-mm-wide ring operating at −1000 V and for the 3-mm-wide ring operating at −2400V. Thus, for the same resolution, the operating voltage of the 4-mm-wide ring is less than half of that for the 3-mm-wide one. The applied voltage for the best energy resolution of 1.36% for the 4-mm-wide ring is smaller than the 1.35% obtained with the 3-mm width. The difference in energy resolution is just 0.01% for an applied voltage difference of 500 V, thus giving the 4-mm Frisch-ring an advantage due to the detector's substantially lower operating voltage.

REFERENCES

[1] S. Del Sordo, L. Abbene, E. Caroli, A. M. Mancini, A. Zappettini, and P. Ubertini, "Progress in the development of CdTe and CdZnTe semiconductor radiation detectors for astrophysical and medical applications," *Sensors*, vol. 9, no. 5, pp. 3491–3526, May 2009.

[2] Y.-L. Liu, J.-Q. Fu, Y.-L. Li, Y.-J. Li, X.-M. Ma, and L. Zhang, "Preliminary results of a Compton camera based on a single 3D position-sensitive CZT detector," *Nucl. Sci. Techn.*, vol. 29, no. 10, p. 145, Oct. 2018.

[3] S. Wang, J.-H. Guo, Y. Zhang, and W. Chen, "High-resolution pixelated CdZnTe detector prototype system for solar hard X-ray imager," *Nucl. Sci. Techn.*, vol. 30, no. 3, p. 42, Mar. 2019.

[4] C. Scheiber and G. C. Giakos, "Medical applications of CdTe and CdZnTe detectors," *Nucl. Instrum. Methods Phys. Res. A, Accel. Spectrom. Detect. Assoc. Equip.*, vol. 458, nos. 1–2, pp. 12–25, Feb. 2001.

[5] A. Owens, M. Bavdaz, H. Andersson, G. Bertuccio, T. Gagliardi, V. Gostillo, I. Lisjutin, S. A. A. Nenonen, A. J. Peacock, H. Sipila, and L. Tröger, "Development of compound semiconductors for planetary and astrophysics space missions," *Proc. SPIE*, vol. 4012, Jul. 2000, pp. 225–236.

[6] A. E. Bolotnikov, S. Babalola, G. S. Camarda, Y. Cui, S. U. Egarievwe, R. Hawrami, A. Hossain, G. Yang, and R. B. James, "Te inclusions in CZT detectors: New method for correcting their adverse effects," *IEEE Trans. Nucl. Sci.*, vol. 57, no. 2, pp. 910–919, Apr. 2010.

[7] N. Zhang, A. Yeckel, A. Burger, Y. Cui, K. G. Lynn, and J. J. Derby, "Anomalous segregation during electrodynamic gradient freeze growth of cadmium zinc telluride," *J. Cryst. Growth*, vol. 325, no. 1, pp. 10–19, Jun. 2011.

[8] A. Hossain, A. E. Bolotnikov, G. S. Camarda, Y. Cui, G. Yang, K.-H. Kim, R. Gul, L. Xu, and R. B. James, "Extended defects in CdZnTe crystals: Effects on device performance," *J. Cryst. Growth*, vol. 312, no. 11, pp. 1795–1799, May 2010.

[9] U. N. Roy, O. K. Okobiah, G. S. Camarda, Y. Cui, R. Gul, A. Hossain, G. Yang, S. U. Egarievwe, and R. B. James, "Growth and characterization of detector-grade CdMnTe by the vertical bridgman technique," *AIP Adv.*, vol. 8, no. 10, Oct. 2018, Art. no. 105012.

[10] S. U. Egarievwe, E. D. Lukosi, R. B. James, U. N. Roy, and J. J. Derby, "Advances in CdMnTe nuclear radiation detectors development," in *Proc. IEEE Nucl. Sci. Symp. Med. Imag. Conf. Proc. (NSS/MIC)*, Sydney, NSW, Australia, Nov. 2018, pp. 1–3.

[11] S. U. Egarievwe, W. Chan, K. H. Kim, U. N. Roy, V. Sams, A. Hossain, A. Kassu, and R. B. James, "Carbon coating and defects in CdZnTe and CdMnTe nuclear detectors," *IEEE Trans. Nucl. Sci.*, vol. 63, no. 1, pp. 236–245, Feb. 2016.

[12] A. Hossain, Y. Cui, A. E. Bolotnikov, G. S. Camarda, G. Yang, D. Kochanowska, M. Witkowska-Baran, A. Mycielski, and R. B. James, "Vanadium-doped cadmium manganese telluride ($Cd_{1-x}Mn_xTe$) crystals as X- and gamma-ray detectors," *J. Electron. Mater.*, vol. 38, no. 8, pp. 1593–1599, Aug. 2009.

[13] Y. Du, W. Jie, T. Wang, Y. Xu, L. Yin, P. Yu, and G. Zha, "Vertical Bridgman growth and characterization of CdMnTe crystals for gamma-ray radiation detector," *J. Cryst. Growth*, vol. 318, no. 1, pp. 1062–1066, Mar. 2011.

[14] J. Lai, J. Zhang, L. Wang, J. Min, W. Wu, M. Shen, and W. Liang, "Comparison of cadmium manganese telluride crystals grown by traveling heater method and vertical Bridgman method," *Crystal Res. Technol.*, vol. 50, no. 11, pp. 817–822, Nov. 2015.

[15] S. U. Egarievwe, M. B. Israel, A. D. Banks, M. L. Drabo, K. L. Dunning, V. J. Cook, F. D. Johnson, S. M. Palmer, U. N. Roy, and R. B. James, "Design and fabrication of a CdMnTe nuclear radiation detection system," in *Proc. SoutheastCon*, Huntsville, AL, USA, Apr. 2019, pp. 1–4.

[16] U. N. Roy, A. E. Bolotnikov, G. S. Camarda, Y. Cui, A. Hossain, K. Lee, W. Lee, R. Tappero, G. Yang, R. Gul, and R. B. James, "High compositional homogeneity of $CdTe_xSe_{1-x}$ crystals grown by the Bridgman method," *APL Mater.*, vol. 3, no. 2, Feb. 2015, Art. no. 026102.

[17] M. Fiederle, D. Ebling, C. Eiche, D. M. Hofmann, M. Salk, W. Stadler, K. W. Benz, and B. K. Meyer, "Comparison of CdTe, $Cd_{0.9}Zn_{0.1}Te$ and $CdTe_{0.9}Se_{0.1}$ crystals: Application for γ- and X-ray detectors," *J. Crystal Growth*, vol. 138, nos. 1–4, pp. 529–533, 1994.

[18] U. N. Roy, G. S. Camarda, Y. Cui, R. Gul, A. Hossain, G. Yang, P. Vanier, V. Lordi, J. Varley, R. B. James, J. Zazvorka, V. Dedic, and J. Franc, "$Cd_{1-x}Zn_xTe_{1-y}$Sey: A potential low-cost alternative to CdZnTe," Brookhaven Nat. Lab., Upton, NY, USA, Tech. Rep. BNL-113882-2017-COPR, 2016.

[19] U. N. Roy, Utpal, G. S. Camarda, Y. Cui, R. Gul, A. Hossain, G. Yang, R. B. James, J. Zázvorka, V. Dedic, and Jan Franc, "Growth and characterization of $Cd_{1-x}Zn_xSe_yTe_{1-y}$ for radiation detector applications," *Proc. SPIE*, vol. 9968, Nov. 2016, Art. no. 99680L.

[20] R. Gul, A. E. Bolotnikov, G. S. Camarda, Y. Cui, S. U. Egarievwe, A. Hossain, U. N. Roy, G. Yang, and R. B. James, "Point defects in $Cd_{1-x}Zn_xTe_{1-y}Se_y$ crystals grown by using Bridgman growth and traveling heater method," *Proc. SPIE*, vol. 9968, Nov. 2016, Art. no. 996815.

[21] R. Gul, U. N. Roy, G. S. Camarda, A. Hossain, G. Yang, P. Vanier, V. Lordi, J. Varley, and R. B. James, "A comparison of point defects in $Cd_{1-x}Zn_xTe_{1-y}Se_y$ crystals grown by Bridgman and traveling heater methods," *J. Appl. Phys.*, vol. 121, no. 12, 2017, Art. no. 125705.

[22] U. N. Roy, G. S. Camarda, Y. Cui, R. Gul, A. Hossain, and G. Yang, "Cadmium zinc telluride selenide (CdZnTeSe): A promising low cost alternative to cadmium zinc telluride (CdZnTe) for medical imaging and nuclear detector applications," Brookhaven Nat. Lab., Upton, NY, USA, Tech. Rep. BNL-113994-2017, Jun. 2017.

[23] U. N. Roy, G. S. Camarda, Y. Cui, R. Gul, A. Hossain, G. Yang, R. B. James, V. Lordi, J. Varley, J. Zazvorka, V. Dedic, and J. Franc, "Crystal growth of CdZnTeSe (CZTS) gamma detectors: A promising alternative to CdZnTe," Brookhaven Nat. Lab., Upton, NY, USA, Tech. Rep. BNL-114158-2017-CP, Aug. 2017.

[24] U. N. Roy, G. S. Camarda, Y. Cui, R. Gul, A. Hossain, G. Yang, R. B. James, V. Lordi, J. Varley, J. Zazvorka, V. Dedic, and J. Franc, "CdZnTeSe: A path forward for room-temperature radiation detector applications," Brookhaven Nat.Lab. (BNL), Upton, NY, USA, Tech. Rep. BNL-114468-2017-CP, Oct. 2017.

[25] U. N. Roy, "$Cd_xZn_{1-x}Te_ySe_{1-y}$ (CZTS): An emerging high-performance gamma-ray detector," Brookhaven Nat. Lab., Upton, NY, USA, Tech. Rep. BNL-203387-2018-INRE, 2018.

[26] N. Utpal Roy, G. Camarda, Y. Cui, R. Gul, G. Yang, B. R. James, J. Zázvorka, V. Dedic, and J. Franc, "CdZnTeSe: An emerging room-temperature semiconductor detector material," *Proc. SPIE*, vol. 10762, Sep. 2018, Art. no. 107620P.

[27] U. N. Roy, G. S. Camarda, Y. Cui, R. Gul, G. Yang, and R. B. James, "Charge-transport properties of as-grown $Cd_{1-x}Zn_xTe_{1-y}Se_y$ by the traveling heater method," *AIP Adv.*, vol. 8, no. 12, Dec. 2018, Art. no. 125015.

[28] M. Rejhon, J. Franc, V. Dědič, J. Pekárek, U. N. Roy, R. Grill, and R. B. James, "Influence of deep levels on the electrical transport properties of CdZnTeSe detectors," *J. Appl. Phys.*, vol. 124, no. 23, Dec. 2018, Art. no. 235702.

[29] S. U. Egarievwe, U. N. Roy, C. A. Goree, B. A. Harrison, J. Jones, and R. B. James, "Ammonium fluoride passivation of CdZnTeSe sensors for applications in nuclear detection and medical imaging," *Sensors*, vol. 19, no. 15, p. 3271, Jul. 2019.

[30] U. N. Roy, G. S. Camarda, Y. Cui, R. Gul, G. Yang, J. Zazvorka, V. Dedic, J. Franc, and R. B. James, "Evaluation of CdZnTeSe as a high-quality gamma-ray spectroscopic material with better compositional homogeneity and reduced defects," *Sci. Rep.*, vol. 9, no. 1, Dec. 2019, Art. no. 1620.

[31] U. N. Roy, G. S. Camarda, Y. Cui, R. Gul, A. Hossain, G. Yang, J. Zazvorka, V. Dedic, J. Franc, and R. B. James, "Role of selenium addition to CdZnTe matrix for room-temperature radiation detector applications," *Sci. Rep.*, vol. 9, no. 1, Dec. 2019, Art. no. 7303.

[32] U. N. Roy, G. S. Camarda, Y. Cui, and R. B. James, "High-resolution virtual Frisch grid gamma-ray detectors based on as-grown CdZnTeSe with reduced defects," *Appl. Phys. Lett.*, vol. 114, no. 23, Jun. 2019, Art. no. 232107.

[33] U. N. Roy, G. S. Camarda, Y. Cui, and R. B. James, "Characterization of large-volume Frisch grid detector fabricated from as-grown CdZnTeSe," *Appl. Phys. Lett.*, vol. 115, no. 24, Dec. 2019, Art. no. 242102.

[34] J. Franc, P. Moravec, V. Dědič, U. Roy, H. Elhadidy, P. Minárik, and V. Šíma, "Microhardness study of $Cd_{1-x}Zn_xTe_{1-y}Se_y$ crystals for X-ray and gamma ray detectors," *Mater. Today Commun.*, vol. 24, Sep. 2020, Art. no. 101014.

[35] S. U. Egarievwe, A. Hossain, I. O. Okwechime, A. A. Egarievwe, D. E. Jones, U. N. Roy, and R. B. James, "Effects of chemical treatments on CdZnTe X-ray and gamma-ray detectors," *IEEE Trans. Nucl. Sci.*, vol. 63, no. 2, pp. 1091–1098, Apr. 2016.

[36] K. Chattopadhyay, M. Hayes, J.-O. Ndap, A. Burger, W. J. Lu, H. G. McWhinney, T. Grady, and R. B. James, "Surface passivation of cadmium zinc telluride radiation detectors by potassium hydroxide solution," *J. Electron. Mater.*, vol. 29, no. 6, pp. 708–712, Jun. 2000.

[37] S. U. Egarievwe, A. Hossain, I. O. Okwechime, R. Gul, and R. B. James, "Effects of chemomechanical polishing on CdZnTe X-ray and gamma-ray detectors," *J. Electron. Mater.*, vol. 44, no. 9, pp. 3194–3201, Sep. 2015.

[38] Y. V. Bezsmolnyy, "Comparative analysis of radiation-sensitive properties of detectors based on CdTe and $Cd_{1-X}Zn_XTe_{1-Y}Se_Y$ single crystals grown by the vertical Bridgman technique," *Nucl. Instrum. Methods Phys. Res. A, Accel. Spectrom. Detect. Assoc. Equip.*, vol. 458, nos. 1–2, pp. 461–463, Feb. 2001.

[39] J. Franc, P. Moravec, V. Dědič, U. Roy, H. Elhadidy, P. Minárik, and V. Šíma, "Microhardness study of Cd1-x ZnxTe1-ySey crystals for X-ray and gamma ray detectors," *Mater. Today Commun.*, vol. 24, Sep. 2020, Art. no. 101014.

[40] D. S. McGregor, Z. He, H. A. Seifert, D. K. Wehe, and R. A. Rojeski, "Single charge carrier type sensing with a parallel strip pseudo-Frisch-grid CdZnTe semiconductor radiation detector," *Appl. Phys. Lett.*, vol. 72, no. 7, pp. 792–794, Feb. 1998.

[41] A. E. Bolotnikov, G. S. Camarda, Y. Cui, S. U. Egarievwe, P. M. Fochuk, M. Fuerstnau, R. Gul, A. Hossain, F. Jones, K. Kim, and O. V. Kopach, "Array of virtual Frisch-grid CZT detectors with common cathode readout and pulse-height correction," *Proc. SPIE*, vol. 7805, Aug. 2010, Art. no. 780504.

[42] J. K. Polack, M. Hirt, J. Sturgess, N. D. Sferrazza, A. E. Bolotnikov, S. Babalola, G. S. Camarda, Y. Cui, S. U. Egarievwe, P. M. Fochuk, R. Gul, A. Hossain, K. Kim, O. V. Kopach, L. Marchini, G. Yang, L. Xu, and R. B. James, "Variation of electric shielding on virtual frisch-grid detectors," *Nucl. Instrum. Methods Phys. Res. A, Accel. Spectrom. Detect. Assoc. Equip.*, vol. 621, nos. 1–3, pp. 424–430, Sep. 2010.

[43] A. E. Bolotnikov, S. Babalola, G. S. Camarda, Y. Cui, S. U. Egarievwe, P. M. Fochuk, M. Hirt, A. Hossain, K. Kim, O. V. Kopach, and N. D. Sferrazza, "Characterization of a 15-mm-long virtual Frisch-grid CZT detector array," *Proc. SPIE*, vol. 7449, Sep. 2010, Art. no. 744909.

[44] N. Zambelli, L. Marchini, G. Benassi, D. Calestani, E. Caroli, and A. Zappettini, "Electroless gold contact deposition on CdZnTe detectors by scanning pipette technique," *J. Instrum.*, vol. 7, no. 8, Aug. 2012, Art. no. P08022.

[45] Q. Zheng, F. Dierre, M. Ayoub, J. Crocco, H. Bensalah, V. Corregidor, E. Alves, R. Fernandez-Ruiz, J. M. Perez, and E. Dieguez, "Comparison of radiation detector performance for different metal contacts on CdZnTe deposited by electroless deposition method," *Crystal Res. Technol.*, vol. 46, no. 11, pp. 1131–1136, Nov. 2011.

[46] G. Montemont, M. Arques, L. Verger, and J. Rustique, "A capacitive Frisch grid structure for CdZnTe detectors," *IEEE Trans. Nucl. Sci.*, vol. 48, no. 3, pp. 278–281, Jun. 2001.

[47] U. N. Roy, S. Weiler, and J. Stein, "Growth and interface study of 2in diameter CdZnTe by THM technique," *J. Cryst. Growth*, vol. 312, no. 19, pp. 2840–2845, Sep. 2010.

[48] A. E. Bolotnikov, J. Butcher, G. S. Camarda, Y. Cui, G. De Geronimo, J. Fried, R. Gul, P. M. Fochuk, M. Hamade, A. Hossain, K. H. Kim, O. V. Kopach, M. Petryk, E. Vernon, G. Yang, and R. B. James, "Array of virtual frisch-grid CZT detectors with common cathode readout for correcting charge signals and rejection of incomplete charge-collection events," *IEEE Trans. Nucl. Sci.*, vol. 59, no. 4, pp. 1544–1551, Aug. 2012.

[49] U. N. Roy, S. Weiler, J. Stein, M. Groza, V. Buliga, and A. Burger, "Charge transport properties of as-grown CZT by traveling heater method," *Nucl. Instrum. Methods Phys. Res. A, Accel. Spectrom. Detect. Assoc. Equip.*, vol. 652, no. 1, pp. 162–165, Oct. 2011.

[50] A. E. Bolotnikov, G. S. Camarda, E. Chen, S. Cheng, Y. Cui, R. Gul, R. Gallagher, V. Dedic, G. De Geronimo, L. Ocampo Giraldo, J. Fried, A. Hossain, J. M. MacKenzie, P. Sellin, S. Taherion, E. Vernon, G. Yang, U. El-hanany, and R. B. James, "CdZnTe position-sensitive drift detectors with thicknesses up to 5 cm," *Appl. Phys. Lett.*, vol. 108, no. 9, Feb. 2016, Art. no. 093504.

STEPHEN U. EGARIEVWE (Member, IEEE) received the B.Sc. degree (Hons.) in engineering physics (nuclear engineering) from Obafemi Awolowo University, Nigeria, the M.Sc. degree in physics and astronomy (solar energy) from the University of Nigeria, the M.S. degree in nuclear engineering from the University of Tennessee, Knoxville, the M.S. degree in computer science from Vanderbilt University, the M.A. degree in physics from Fisk University, the M.S. degree in computer science from Nova Southeastern University, and the Ph.D. degree in applied physics from Alabama A&M University.

He has served as the immediate Former Chair of the Department of Engineering, Construction Management, and Industrial Technology, Alabama A&M University. His prior appointments include: an Assistant and an Associate Professorships at Fisk University, a Lecturer-I at Usmanu Danfodiyo University, Nigeria, an Assistant Lecturer at Ambrose Alli University, Nigeria, and a Laboratory Assistant at the University of Nigeria. He was a SLAC Scholar and an ABET-IDEAL Scholar. He is also the Director of the Nuclear Engineering and Radiological Science Center and a Professor with the Department of Electrical Engineering and Computer Science, Alabama A&M University. He has been serving as the Guest Scientist of the Brookhaven National Laboratory, since 2008. He has authored one book and coauthored more than 100 scientific publications. His current research interests include nuclear security and safety, materials science, nanotechnology, data analytics and visualization, the Internet-based remote laboratory instrumentation, petroleum and gas workforce, and STEM education.

Dr. Egarievwe is a member of the Society of Petroleum Engineers (SPE). He is also the National Secretary of the Interdisciplinary Consortium for Research and Educational Access in Science and Engineering (InCREASE), USA. He received the Research and Development 100 Award from R&D Magazine. He has served as a Co-Editor of one book.

UTPAL N. ROY received the M.Sc. degree in physics, the M.Tech. degree in materials science (semiconductor), and the Ph.D. degree in materials science (semiconductor) from IIT Kharagpur.

He currently works as the Senior Advisory Scientist of the DOE's Savannah River National Laboratory. His prior appointments include: a Scientist at the Brookhaven National Laboratory, Upton, NY; a Physicist at FLIR (Formerly ICx) Radiation Inc., Oak Ridge, TN; and a Research Associate at Fisk University, Nashville, TN. He has coauthored about 120 publications in peer reviewed journals, and one patent. His research interests include basic and applied materials research devoted to lasers hosts, semiconductor materials, radiation detector materials, and detector systems. His current research interest includes development of new materials for radiation detector applications. He was a co-recipient of two Research and Development 100 Awards and two times Research and Development 100 Finalist from R&D Magazine Innovator of the Year.

EZEKIEL O. AGBALAGBA was born in Agbarha-Otor, Delta State, Nigeria. He received the B.Sc. degree in pure and applied physics from Delta State University, Abraka, Nigeria, in 2000, the M.Sc. degree in environmental radiation physics, in 2007, and the Ph.D. degree in nuclear and radiation physics from the University of Port Harcourt, Nigeria, in 2012.

From 2003 to 2010, he has lectured at the Bayelsa State College of Arts and Science, Yenagoa, Bayelsa State, Nigeria, and has served as a Research Assistant with the University of Port Harcourt. He is currently a certified Nuclear Security Specialist in radionuclides waste security management with the World Institute of Nuclear Security, Australia. He is also an Associate Professor of nuclear and radiation health physics with the Federal University of Petroleum Resources, Effurun, Nigeria. He has authored three books and four book chapters. He has coauthored over 60 scientific articles in learned reputable international and local journals. He has presented and coauthored over 40 papers in conferences.

BENICIA A. HARRISON was born in Mobile, AL. She received the B.S. degree in biology from Alabama Agricultural and Mechanical University, Huntsville, AL, in 2020. She is currently pursuing the M.D. degree at the College of Medicine, University of South Alabama, Mobile, AL.

From 2016 to 2020, she was a Research Assistant with the Forestry Department and the Biological and Environmental Sciences Department, Alabama Agricultural and Mechanical University. In the summer of 2018, she has worked as an Intern with the Brookhaven National Laboratory due to her interest in the clinical uses of radiation detectors. Her current research interests include microbiology and immunology.

CARMELLA A. GOREE was born in Detroit, MI, in 1997. She received the B.S. degree in biology from Alabama A&M University, Huntsville, AL, in 2020. She plans to pursue graduate studies in public health.

As an undergraduate, she participated in many research projects, including doing a study on the relationship between social factors, behavior, and neighborhood level indicators among teens with asthma. She conducted research at the Brookhaven National Laboratory, Upton, NY, where she worked on radiation sensors for applications in nuclear detection and medical imaging. She also conducted research at the University of California at Los Angeles on antibiotic resistance. While at Alabama A&M University, she led multiple projects and represented the university at several research conferences in AL and Washington, DC. Her research interests include the field of public health and medicine.

EMMANUEL K. SAVAGE is currently pursuing the bachelor's degree with Alabama A&M University, Huntsville, AL, where he is a double major in physics and criminal justice. He has served as a Summer Intern at Apple and the Brookhaven National Laboratory, Upton, NY. At the Brookhaven National Laboratory, he has worked on radiation sensors for applications in nuclear and radiological threat detection, gamma-ray spectroscopy, astrophysics, and medical imaging. He also participated in research activities at Alabama A&M University. His professional research interest includes forensic science.

RALPH B. JAMES (Fellow, IEEE) received the B.S. degree in engineering physics from the University of Tennessee, the M.S. degree in physics from Georgia Tech, and the M.S. and Ph.D. degrees in applied physics from Caltech. He currently serves as the Associate Laboratory Director for Science and Technology and the Chief Research Officer with the DOE's Savannah River National Laboratory. He has coauthored more than 650 scientific publications and holds 27 patents. His research interests include basic and applied research devoted to semiconductor materials, radiation detectors, and imaging systems.

Dr. James is a Fellow of the IEEE, SPIE, AAAS, OSA, MRS and APS. He has received numerous international honors for his work on detectors and imaging, including the Discover Magazine Innovator of the Year, seven Research and Development 100 Awards, the IEEE Outstanding Radiation Instrumentation Award, the IEEE Harold Wheeler Award, the Room-Temperature Semiconductor Scientist Award, the Battelle Innovation Award, the Frost and Sullivan Invention of the Year in prostate cancer, the Long Technology Hall of Fame Inductee, among many others. He has served as an Editor for 34 books.